Bulletin of the New Zealand Society for Earthquake Engineering, Vol. 59, No. 1, March 2026

PREDICTION OF ECONOMIC LOSSES FROM EARTHQUAKES IN MAINLAND CHINA

Chenhui Wang[1], Xiaoshan Wang[2*], Guojun Lv[3], Xiaotao Zhang[4], Libing Wang[5] and Na Luo[6]

(Submitted *March 2025*; Reviewed *April 2025*; Accepted *June 2025*)

ABSTRACT

After an earthquake, the rapid assessment of economic losses enables government agencies to accurately evaluate the severity of the disaster, thereby initiating the appropriate level of emergency response in a timely manner. By analysing the scope of the affected area and the scale of property losses, rescue resources can be rationally allocated to the most severely impacted regions, thereby effectively mitigating the losses caused by the disaster, while securing valuable time for emergency rescue and disaster relief efforts. To address the challenges in predicting earthquake economic losses, including numerous influencing factors, high computational demands, and complex model training, this study develops a Support Vector Machine (SVM) model optimized by Principal Component Analysis (PCA) and Genetic Algorithm (GA). PCA reduces the dimensionality of economic loss-related factors by eliminating redundancy, selecting principal components with high contribution rates as SVM inputs, with economic loss as the output. GA optimizes SVM performance parameters to establish the PCA-GA-SVM model. Testing on sample data shows it outperforms GA-SVM, GA-BP (Genetic Algorithm-optimized Back-Propagation neural network), and PCA-GA-BP models, achieving an average prediction accuracy of 95.94%, with a mean absolute percentage error (*MAPE*) of 4.0522%, normalized root mean square error (*NRMSE*) of 2.361%, and coefficient of determination (R^2) of 0.9994. These results underscore the model's accuracy and generalization ability, making it an effective tool for rapid, reliable earthquake loss prediction.

https://doi.org/10.5459/bnzsee.1747

INTRODUCTION

Situated between the Pacific Rim and Eurasian seismic zones, China experiences some of the highest frequencies and severities of continental earthquakes globally, driven by its unique tectonic setting, accounting for 33% of such events despite comprising only 7% of the world's land area. Earthquakes of varying magnitudes occurring annually pose significant risks to lives and property at both national and individual levels. For instance, the 1976 Tangshan earthquake (magnitude 7.8) in Hebei resulted in direct economic losses exceeding 10 billion yuan and a casualty toll of 400,000, including 240,000 deaths, while the 2008 Wenchuan earthquake (magnitude 8.0) claimed 80,000 lives and caused over 800 billion yuan in direct economic losses. Following an earthquake, government agencies must swiftly mobilize personnel and resources for rescue efforts. Understanding the disaster's scope and assessing basic conditions are critical priorities, among which the evaluation of economic losses plays a key role [1-6].

Research on earthquake loss assessment originated in the United States, with Freeman pioneering regional loss studies in 1932, exploring the relationship between seismic damage and insurance [7]. In China, following the 1989 Datong earthquake (magnitude 6.1), the China Earthquake Administration deployed experts to apply scientific methods, yielding reliable disaster assessment outcomes. Subsequently, the agency developed a series of guidelines and protocols, continuously refining seismic damage assessment techniques through standardized protocols and empirical studies. In recent years, experts worldwide have advanced post-earthquake loss assessment, proposing various methods to evaluate economic losses from seismic events, with the most common approaches including the following:

(1) Vulnerability Classification List Method

The vulnerability classification list method, introduced by Algermissen (1984), was a widely used approach valued for its simplicity and suitability for precise loss estimation [8]. Xu (2008) applied it to assess Wenchuan earthquake losses, achieving reliable results in Sichuan and Gansu [9], though its effectiveness depends on detailed building data due to the unpredictable locations of destructive earthquakes [10].

(2) GDP-based Economic Indicator Method

Chen (1999) proposed using macroeconomic indicators for loss prediction when detailed data are unavailable, relying on socioeconomic statistics [11]. Liu (2010) developed a rapid assessment tool using these indicators, capable of generating automated disaster reports, which effectively captured key features of Tianjin's "Tenth Five-Year" emergency system outcomes [12]. While Fan (2016) combined GDP with a macro-vulnerability model to successfully assess losses in Zhangjiakou, Hebei [13].

(3) Remote Sensing Imagery and GIS-based Method

Advances in remote sensing and GIS technology have opened new avenues for loss assessment. Badal (2005) modelled local wealth as a function of GDP, leveraging GIS to analyse spatial data and link seismic intensity to economic losses (as a percentage of wealth) [14]. Wang (2007) enhanced automation in damage extraction using these technologies [15]. Zhou (2013) developed a GIS-based system, delivering accurate

[1] *Intermediate Research Engineer, Hongshan Natl Observ Thick Sediments & Seism Hazar, China, Email: Caesar621@163.com*
[2] *Corresponding Author, Hebei Earthquake Agency, China, Email: wangxsh2022@163.com.*
[3] *Senior Research Engineer, Hebei Earthquake Agency, China, Email: 328293676@qq.com.*
[4] *Senior Research Engineer, Hebei Earthquake Agency, China, Email: 249595254@qq.com.*
[5] *Senior Research Engineer, Hebei Earthquake Agency, China, Email: 276877415@qq.com.*
[6] *Senior Research Engineer, Hebei Earthquake Agency, China, Email: 93640348@qq.com.*

results in practical applications [16]. Lu (2021) employed drone-based remote sensing to analyse building structures and seismic resistance, improving efficiency in pre-assessment tasks [17].

Despite their merits, these methods face challenges: The vulnerability classification method requires detailed building classifications to construct damage matrices, with greater detail yielding more precise results, though collecting and updating such data is labour-intensive and challenging in practice. Field surveys are similarly time-consuming and resource-heavy. The economic indicator method may produce errors due to discrepancies between calculated and actual GDP data. Remote sensing imagery, while valuable, is weather-dependent and has acquisition limitations. These challenges highlight the need for faster, more effective assessment approaches.

With the rise of machine learning, support vector machines (SVMs) have shown strong performance in handling small-sample, nonlinear problems, quickly gaining traction in seismic disaster mitigation research. Zhao used Sichuan as a case study, proposed an integrated SVM and XGBoost model, employing feature selection, Bayesian optimization, and SHAP analysis to predict GDP-related losses rapidly and transparently [18]. Zhang developed an image classification method integrating scale-invariant feature transform and SVM algorithms, enabling accurate identification of building damage via drone remote sensing, validated during the 2021 Yangbi earthquake [19]. Building on these advances, this study introduces a seismic economic loss prediction model optimizing SVM with principal component analysis (PCA) and genetic algorithms (GA). PCA reduces the dimensionality of loss-influencing factors, simplifying SVM complexity, while GA optimizes SVM parameters, establishing a PCA-GA-SVM model to support post-earthquake emergency response.

BASIC PRINCIPLE

Principal Component Analysis

The fundamental concept of the Principal Component Analysis (PCA) method is to transform the original variables into a new set of linearly independent composite variables. Based on practical requirements, a subset of these composite variables is selected according to their cumulative contribution rates to capture as much information as possible from the original variables [20-22]. The specific steps are as follows:

Let $(X_1, X_2, \ldots Xn)$ represent the n earthquake samples in the overall dataset $\boldsymbol{X}$ of earthquake economic losses. Each sample consists of m-dimensional variables, corresponding to m indicators of economic losses from earthquakes, and the corresponding matrix is:

$$X_{m\times n} = \begin{bmatrix} x_{11} & x_{12} & \cdots & x_{1n} \\ x_{21} & x_{22} & \cdots & x_{2n} \\ \vdots & \vdots & \ddots & \vdots \\ x_{m1} & x_{m2} & \cdots & x_{mn} \end{bmatrix} \tag{1}$$

(1) To eliminate the impact of dimensional differences between various indicators, the original data is standardized by the following formulas:

$$zx_{ij} = \frac{x_{ij} - \bar{x_{ij}}}{\sqrt{\mathrm{var}(x_j)}} \tag{2}$$

$$\mathrm{var}(x_j) = \frac{1}{n-1}\sum_{i=1}^{n}\left(x_{ij} - \bar{x_j}\right)^2 \tag{3}$$

$$\bar{x_j} = \frac{1}{n}\sum_{i=1}^{n} x_{ij} \tag{4}$$

(2) Next, the covariance matrix of the data is calculated, and then it is converted into a correlation matrix according to the following formula:

$$\rho_{ij} = cov(X_i, X_j) \Big/ \sqrt{\sigma_{ii}\sigma_{jj}} \tag{5}$$

(3) The eigenvalues of the correlation matrix are calculated as $\lambda_1 \geq \lambda_2 \geq \ldots \lambda_m \geq 0$. Then the orthogonal unit eigenvectors corresponding to the eigenvalues are obtained: $\boldsymbol{e}_1, \boldsymbol{e}_2, \cdots, \boldsymbol{e}_m$.

(4) The i-th principal component of the m-dimensional variables is determined as $Y_i = \boldsymbol{e}_i^T \boldsymbol{X} = \boldsymbol{e}_{1i}x_1 + \boldsymbol{e}_{2i}x_2 + \cdots + \boldsymbol{e}_{mi}x_m$, and the contribution rate of this component is λ_i / P , where i=1,2,3…m, $\mathrm{P} = \sum_{i=1}^{m}\lambda_i$, and the cumulative contribution rate of the first q principal components is $\sum_{i=1}^{q}\lambda_i$ / P .

In practical applications, principal components with low contribution rates are often omitted. If the cumulative contribution rate of the first n components exceeds 85%, only the first n components are used as input variables for the SVM model.

Support Vector Machine

Support Vector Machine (SVM) is a statistical learning method based on the principle of structural risk minimization, aimed at constructing the optimal hyperplane. The core idea is to map input samples to a higher-dimensional feature space through a nonlinear transformation, converting the nonlinearly separable problem in the original sample space into a linearly separable one in the feature space. This method demonstrates excellent generalization capability when handling statistical learning problems involving small samples, nonlinearity, and high-dimensional data [23-24]. The core concept is outlined as follows:

Let the newly generated principal component sample set be denoted as (X_i, y_i), $i = 1,2\ldots n$,where $X_i \in R^n$ is the input vector, and $y_i \in R$ is the corresponding output, representing the economic loss from an earthquake. Let $\phi(X_i)$ represent the principal component sample data mapped into the high-dimensional space, and ϕ denote the corresponding nonlinear mapping. The resulting function expression is given by:

$$y_i = W \cdot \phi(X_i) + b \tag{6}$$

Where W represents the adjustable weight vector, b is the bias term, and both W and b are n-dimensional vectors. The goal is to find the optimal classification hyperplane, which involves determining the best values for w and b. Considering the presence of fitting errors, ξ and ξ^* are introduced as slack variables. Following the principle of structural risk minimization, the ε-SVR model is used to establish the constrained optimization function for the model:

$$\min_{W,b,\xi,\xi^*} \frac{1}{2}W^TW + C\sum_{i=1}^{m}(\xi_i + \xi_i^*)$$
$$s.t \begin{cases} y_i - W^T\phi(X_i) + b \le \varepsilon + \xi_i^*, \\ W^T\phi(X_i) + b - y_i \le \varepsilon + \xi_i, \\ \xi_i, \xi_i^* \ge 0 \end{cases} \quad (7)$$
$$(i = 1, \cdots, m)$$

The purpose of using $\frac{1}{2}W^TW$ is to enhance the generalization ability of the function, making it smoother. The addition of $C\sum_{i=1}^{m}(\xi_i + \xi_i^*)$ helps to reduce the variations caused by certain outliers in the model. Where C is the penalty parameter, which represents the weight of outliers and is used to adjust the penalty for data points that exceed the fitting error ε. A larger C indicates that outliers have a greater influence on the objective function. Equation (7) is a convex quadratic optimization problem, which is solved using the Lagrange multiplier method to establish the Lagrange function:

$$\begin{aligned} &L(W, b, \xi, \xi^*, a, a^*, r, r^*) = \\ &\frac{1}{2}W^TW + C\sum_{i=1}^{m}(\xi_i + \xi_i^*) - \sum_{i=1}^{m}a_i^*(y_i \\ &-W^T \cdot \phi(X_i) - b - \varepsilon - \xi_i^*) - \sum_{i=1}^{m}a_i \\ &(W^T \cdot \phi(X_i) + b - y_i - \varepsilon - \xi_i) - \\ &\sum_{i=1}^{m}r_i - \sum_{i=1}^{m}r_i^* \end{aligned} \quad (8)$$

Where a, a^*, r and r^* are Lagrange multipliers.

Taking the partial derivatives of Equation (8) with respect to W and b, setting them to zero, and substituting them back into Equation (8) and yields the dual form of the problem. The corresponding Karush-Kuhn-Tucker (KKT) conditions are then identified, and a quadratic programming optimization algorithm is applied iteratively as the training method. This process determines the optimal multiplier a_i^{new} corresponding to parameters a_i and a_i^*, while also constructing the predictive function:

$$f(X_i) = \sum_{i=1}^{m}(a_i^* - a_i)\phi(X_i)^T\phi(X_i) + b \quad (9)$$

In this equation, $f(X_i)$ represents the predicted economic loss caused by an earthquake. The terms a_i^* and a_i are Lagrange multipliers. $\phi(X_i)^T\ \phi(X_i)$ denotes the kernel function, while X_i refers to the newly generated principal components.

Determining the exact form of a nonlinear mapping is challenging. Therefore, kernel functions are introduced to transform the inner product of the original features into an equivalent form in the mapped feature space, thus indirectly solving the nonlinear mapping. Kernel functions that satisfy Mercer's theorem are considered valid. Among these, the Radial Basis Function (RBF) kernel ($K(X_i, X_j) = \exp\left(g\left\|X_i - X_j\right\|^2\right)$) is widely used due to its broad convergence domain and is typically the most common choice for solving practical problems.

The accuracy and precision of SVM regression depend on the values of the penalty factor C and the radial basis function radius g. Traditional support vector machine determines these parameters based on empirical selection, which often results in suboptimal accuracy. To address this, this study employs a genetic algorithm to optimize the parameter selection for SVM.

Genetic Algorithm Optimization of SVM

The genetic algorithm is primarily used to find optimal solutions by simulating biological evolution. The process begins with encoding the problem for computation and defining a fitness function. Next, an initial population of candidate solutions is generated randomly, and their fitness values are evaluated. Based on the principles of natural selection, the fittest individuals are chosen. Finally, genetic operators refine the selection to determine the optimal parameters. The GA is applied to optimize the SVM parameters C and g. This optimization process enhances the accuracy of the support vector machine, ensuring optimal results [25-26].

Model Development Process

The earthquake economic loss prediction model is built on PCA and GA-SVM. The model development process based on PCA-GA-SVM is as follows:

Step 1: Apply Principal Component Analysis (PCA) to reduce the dimensionality of the raw data and normalize it. The normalized, dimension-reduced data is then used as input for the GA-SVM model.

Step 2: Use the Genetic Algorithm (GA) to optimize the parameters of the Support Vector Machine (SVM). Train the GA-SVM model with learning samples to search for the optimal SVM parameters C and g.

Step 3: Develop the PCA-GA-SVM model for earthquake economic loss prediction. Test the model using sample data and compare its predictions with those of other models.

Step 4: Analyse and compare the prediction accuracy of different models to draw conclusions.

The PCA-GA-SVM model prediction process is illustrated in Figure 1.

Model Evaluation Metrics

In predictive modelling, common evaluation metrics include Mean Absolute Percentage Error (*MAPE*), Root Mean Square Error (*RMSE*), and the Coefficient of Determination (R^2). RMSE primarily assesses the stability of predictions, while MAPE and R^2 measure prediction accuracy. The closer the R^2 value is to 1, the more accurate the model. Lower values for the other metrics indicate greater stability and accuracy in the predictive model.

$$MAPE = 100 \times \frac{1}{K}\sum_{k=1}^{K}\left|(\eta_k - \hat{\eta}_k)/\eta_k\right| \quad (10)$$

$$RMSE = \sqrt{\sum_{k=1}^{K}(\eta_k - \hat{\eta}_k)^2 / K} \quad (11)$$

$$R^2 = \frac{(K\sum_{k=1}^{K}\eta_k\hat{\eta}_k - \sum_{k=1}^{K}\eta_k\sum_{k=1}^{K}\hat{\eta}_k)^2}{[K\sum_{k=1}^{K}\hat{\eta}_k^{\,2} - (\sum_{k=1}^{K}\hat{\eta}_k)^2][K\sum_{k=1}^{K}\eta_k^{\,2} - (\sum_{k=1}^{K}\eta_k)^2]} \quad (12)$$

Where η_k is the actual value and $\hat{\eta}_k$ is the predicted value.

To provide a relative measure of prediction error, we also compute the Normalized RMSE (NRMSE), defined as:

$$NRMSE = \frac{RMSE}{\bar{\eta}}, \text{ where } \bar{\eta} = \frac{1}{K}\sum_{k=1}^{K}\eta_k$$

NRMSE represents the prediction error as a fraction of the average economic loss, offering a more intuitive perspective on model performance.

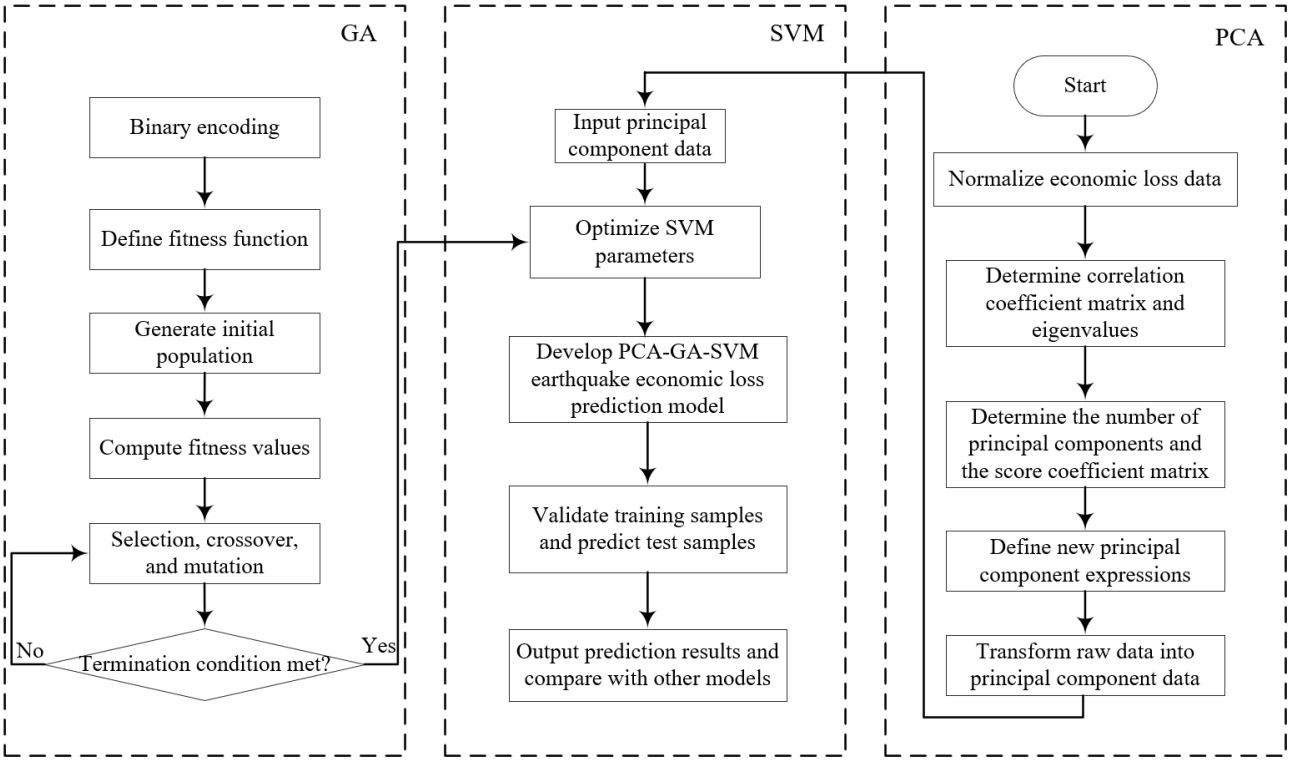

Figure 1: The flow chart of PCA-GA-SVM.

MODEL BUILDING AND PREDICTION

Impact Indicator Analysis

Economic losses from earthquakes result from a combination of multiple factors, necessitating a comprehensive evaluation of various indicators to accurately assess post-earthquake economic impacts [27-32]. To enable rapid assessment of these losses, this study selects five key indicators with significant influence: earthquake magnitude, epicentral intensity, seismic fortification intensity, per capita GDP, and population density. These indicators are closely tied to the economic losses triggered by earthquakes and effectively capture the varying degrees of disaster impact across different regions. Magnitude and epicentral intensity reflect the strength and source characteristics of an earthquake; higher magnitude and greater epicentral intensity correspond to increased energy release and destructive power, leading to larger economic losses under similar conditions. Seismic fortification intensity, on the other hand, indicates the earthquake resistance of buildings. Stronger fortification enhances a structure's ability to withstand seismic damage, thereby reducing the scale of economic losses. Per capita GDP and population density provide insights into a region's socioeconomic conditions, reflecting its economic development and population concentration. Generally, under equivalent earthquake conditions, more developed regions experience greater economic losses. This occurs because higher development levels correlate with denser populations, concentrated lifeline infrastructure, and extensive above- and below-ground utility networks. Consequently, regions with higher per capita GDP and population density possess greater economic foundations and development levels, resulting in more affected individuals, larger societal wealth exposure, and amplified economic losses under comparable seismic impacts [33-39].

Data Sources and Preprocessing

The earthquake disaster data utilized in this study are sourced from the *Compilation of Earthquake Disaster Loss Assessment Reports for Mainland China*, 1996–2015 (*China Earthquake Administration, Department of Monitoring and Prediction*, 2015). This analysis draws on a statistical sample of 37 earthquakes in mainland China from 1996 to 2014. Given the extended time span of these events, factors such as economic growth, population increases, and changes in price indices must be considered when evaluating their economic impacts. Economic losses for each earthquake were originally recorded at the price levels of their respective years; however, varying price levels across years obscure the true relationship between losses over time. To address this, adjustments are necessary to eliminate differences arising from changes in the real value of monetary units due to economic development, enabling a consistent comparison of losses at comparable prices. The growth rate of per capita GDP serves as a macroeconomic indicator of economic development speed in mainland China, offering a critical reference for longitudinally comparing regional economic levels over time. Using per capita GDP growth rates from 1996 to 2014, all loss figures were standardized to 2014 comparable prices. This adjustment facilitates statistical analysis of earthquake economic losses based on 2014 values. Leveraging these data, a model was constructed and analysed using the 37 sample events, with details provided in Table 1. Where S_1 represents earthquake magnitude, S_2 denotes epicentral intensity, and S_3 indicates seismic design intensity. S_4 represents per capita GDP (in 10,000 CNY) adjusted to 2014 constant prices, S_5 denotes population density (persons per km²), and the final column provides economic losses (in 10,000 CNY) standardized to 2014 prices.

Table 1: Original seismic sample data.

Serial number	Date	Location	S_1	S_2	S_3	S_4	S_5	Economic losses (in 10,000 CNY)
1	1996-05-03	Baotou	6.4	8	8.0	0.8969	480.2	268300.0
2	1996-02-03	Lijiang	7.0	9	10	0.2200	46.70	304900.0
3	1998-01-10	Zhangbei	6.2	8	9.0	0.1900	87.80	83600.00
4	1998-05-29	Pishan	6.2	7	7.0	0.0700	5.200	5486.750
5	1998-11-19	Ning'er	6.2	8	9.0	0.1000	38.60	50314.00
6	2000-01-15	Yao'an	6.5	8	9.0	0.2900	123.0	106621.0
7	2000-01-27	Qiubei	5.5	7	8.0	0.1200	0.1200	10374.00
8	2001-04-12	Shidian	5.9	8	8.0	0.2400	161.0	50490.00
9	2001-05-24	Yanyuan	5.8	7	7.0	0.1500	37.00	14934.00
10	2001-10-27	Yongsheng	6.0	7	6.0	0.2100	74.00	41050.00
11	2002-12-14	Yumen	5.9	7	7.0	0.5000	14.00	7020.000
12	2003-02-24	Bachu	6.8	9	11	0.2800	17.00	139792.0
13	2003-07-21	Dayao	6.2	8	9.0	0.3500	68.00	59190.00
14	2003-08-16	Balinzuoqi	5.9	8	10	0.2400	54.00	80649.00
15	2003-10-01	Dayao	6.1	8	9.0	0.3500	68.00	41560.00
16	2003-10-25	Minle	6.1	8	9.0	0.4300	81.00	50140.00
17	2004-03-24	Balinzuoqi	5.9	7	8.0	0.5600	3.000	20272.00
18	2004-08-10	Ludian	5.6	8	9.0	0.1400	243.0	33226.00
19	2005-08-05	Huize	5.3	6	4.0	0.7600	109.0	16998.00
20	2005-11-26	Jiujiang	5.7	7	8.0	0.4600	278.0	203759.0
21	2007-06-03	Ning'er	6.4	8	9.0	0.5600	104.0	189860.0
22	2007-07-20	Tekesi	5.7	7	6.0	0.3100	27.00	11060.00
23	2008-08-21	Yingjiang	5.9	8	9.0	0.6700	79.00	130800.0
24	2008-08-30	Renhe	6.1	8	9.0	3.140	325.0	446187.0
25	2008-10-06	Dangxiong	6.6	8	7.0	0.8800	3.000	41137.00
26	2009-07-09	Yao'an	6.0	8	9.0	0.7600	115.0	215400.0
27	2011-03-10	Yingjiang	5.8	8	9.0	1.030	59.00	238480.0
28	2011-06-20	Tengchong	5.2	6	4.0	1.100	139.0	27840.00
29	2011-08-11	Jiashi	5.8	7	6.0	0.8100	24.00	18322.00
30	2012-06-30	Xinyuan	6.6	8	8.0	2.090	17.00	199032.0
31	2012-09-07	Yiliang	5.7	8	9.0	0.7000	177.0	477104.0
32	2013-01-18	Baiyu	5.4	7	7.0	1.280	5.000	12099.00
33	2013-04-20	Lushan	7.0	9	11	2.050	165.0	6032378
34	2013-07-22	Minxian	6.6	8	8.0	0.5000	144.0	1758800
35	2013-08-12	Zuogong	6.1	8	9.0	1.130	5.000	270715.0
36	2014-10-07	Jinggu	6.6	8	9.0	2.380	48.00	511020.0
37	2014-11-22	Kangding	6.3	8	7.0	3.620	17.00	269203.0

Principal Component Analysis

Principal component analysis (PCA) was conducted on the original data using SPSS, with corresponding results from the Kaiser-Meyer-Olkin (*KMO*) test and Bartlett's test of sphericity presented in Table 2. The results show a *KMO* value greater than 0.5 and a significance level below 0.05, indicating strong correlations among the influencing indicators and justifying the application of factor analysis.

Factor analysis yielded the contribution rates of each principal component, as shown in Table 3. According to Table 3, the cumulative contribution rate of the first four principal components reaches 97.635%, effectively capturing the information from the original data while reducing dimensionality and enhancing model efficiency.

The coefficient matrix of principal component scores is provided in Table 4. From Table 4, it is evident that earthquake magnitude, epicentral intensity, and seismic design intensity predominantly influence principal component $F1$, while per capita GDP and population density have a greater impact on $F2$. Population density significantly affects $F3$, and per capita GDP strongly influences $F4$. The expressions for the principal components are given in Equation (13).

Table 2: KMO test and bartlett's sphericity test results.

KMO Sampling Adequacy		0.5240
Bartlett's Sphericity Test	Approximate Chi-Square	64.763
	Degrees of Freedom	10.000
	Significance	0.000

Table 3: Eigenvalues, contributions of principal components and cumulative contributions.

Principal Component	Eigenvalue	Contribution Rate (%)	Cumulative Contribution Rate (%)
$F1$	2.288	45.768	45.768
$F2$	1.138	22.757	68.524
$F3$	0.972	19.442	87.966
$F4$	0.483	9.6690	97.635
$F5$	0.118	2.3650	100.00

Table 4: Score coefficient matrix of principal components.

Impact Indicator	Principal Components			
	$F1$	$F2$	$F3$	$F4$
magnitude	0.371	0.058	-0.290	-0.844
epicentral intensity	0.421	-0.020	-0.010	-0.075
seismic design intensity	0.335	-0.306	0.279	0.927
GDP per capita	0.082	0.747	-0.396	0.634
population density	0.060	0.472	0.843	-0.301

$$\begin{aligned} F1 &= 0.371S_1 + 0.421S_2 + 0.335S_3 + 0.082S_4 + 0.060S_5 \\ F2 &= 0.0580S_1 - 0.020S_2 - 0.306S_3 + 0.747S_4 + 0.472S_5 \\ F3 &= -0.290S_1 - 0.010S_2 + 0.279S_3 - 0.396S_4 + 0.843S_5 \\ F4 &= -0.844S_1 - 0.075S_2 + 0.927S_3 + 0.634S_4 - 0.301S_5 \end{aligned} \tag{13}$$

Using Equation (13), the dimensionality-reduced principal component data were derived, as presented in Table 5.

Table 5: Dimensionality-reduced principal component data.

	*F*1	*F*2	*F*3	*F*4
1	34.62795	227.5356	402.5174	-149.9730
2	9.541040	22.12674	37.43998	-19.57320
3	11.28678	41.47713	72.34116	-31.21310
4	5.564940	2.726290	2.487880	-7.278620
5	8.327400	18.18750	30.90120	-16.46100
6	13.51828	58.18363	101.8882	-41.99810
7	5.339540	0.019280	-1.332360	-4.200040
8	15.23658	76.35348	133.8370	-53.88840
9	7.331100	17.77245	29.37960	-16.46210
10	9.295220	35.59887	60.20984	-28.65690
11	6.016900	7.183700	9.823000	-9.401600
12	8.024760	7.835560	12.71612	-9.499680
13	10.11190	32.25105	55.58640	-25.15190
14	9.486580	25.23748	44.19396	-19.82740
15	10.07480	32.24525	55.61540	-25.06750
16	10.86136	38.44101	66.54272	-28.92980
17	5.696820	1.730520	0.805240	-5.125560
18	20.37208	114.6594	203.3686	-77.45360
19	10.42462	52.81512	89.43104	-39.10440
20	22.11442	131.4442	232.7278	-87.79520
21	12.36332	49.41152	85.79324	-36.02360
22	6.372120	13.47217	20.63624	-14.19330
23	10.68684	37.66469	64.81968	-28.00680
24	25.72358	155.6334	271.1616	-100.6560
25	5.733760	2.602160	-0.092480	-7.442480
26	12.89132	54.72972	95.10304	-38.87020
27	9.479260	28.48781	47.84612	-21.67420
28	12.21540	67.22330	114.6154	-47.83440
29	6.270220	12.43547	17.88024	-13.05770
30	7.007980	9.808030	11.50936	-9.962340
31	16.49674	83.94644	147.4719	-57.30430
32	5.355360	3.489360	2.072120	-5.776080
33	17.12410	79.02535	136.7212	-53.09430
34	14.49760	68.56430	119.2000	-49.19740
35	6.358760	3.091910	2.197520	-5.609980
36	9.226760	24.35066	37.80652	-18.18250
37	6.687140	11.23954	10.71148	-9.666120

Training the PCA-GA-SVM Model

The four linearly independent principal components were used as input vectors for the support vector machine (SVM), with earthquake economic loss as the output vector. All 37 earthquake samples were employed to optimize the hyperparameters (C and g) of the support vector machine model using a genetic algorithm, ensuring robust parameter selection for enhanced predictive performance.

For the predictive model, a radial basis function was chosen as the SVM kernel. A genetic algorithm (GA) was implemented in MATLAB to optimize SVM parameters. The GA parameters were set as follows: population size of 20, maximum number of generations of 100, crossover rate of 0.8, and mutation rate of 0.1. The crossover rate of 0.8 ensures sufficient diversity in the population, while the mutation rate of 0.1 helps avoid local optima without overly disrupting convergence. These values were determined through preliminary experiments, where different combinations of crossover and mutation rates were tested to minimize the SVM's prediction error (measured by MAPE on the validation set). The GA optimization process is illustrated in Figure 2.

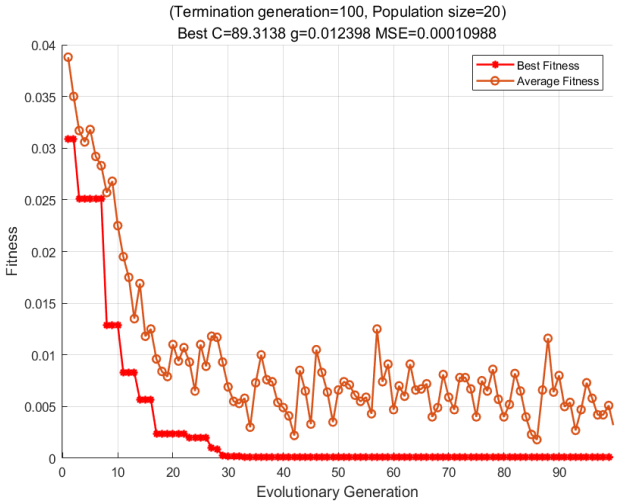

Figure 2: Optimization process of GA.

As shown in Figure 2, the best fitness value stabilized after 30 generations, exhibiting minor fluctuations and a small gap from the average fitness. This indicates rapid convergence and good fitness quality. The optimal parameters obtained were C = 89.3138 and g = 0.012398, with a mean squared error (MSE) of 0.00010988 on the fitness curve, reflecting high parameter accuracy.

Prediction Results Analysis

To ensure the generalization ability and validate the effectiveness and reliability of the PCA-GA-SVM model, we incorporated the optimal parameters (C = 89.3138, g = 0.012398) into the SVM model and employed 5-fold cross-validation for calibration and performance evaluation. Specifically, the principal component dataset was divided into five subsets (three subsets with seven samples each and two subsets with eight samples each). In each iteration, four subsets were used for training, and the remaining subset was used for testing, with the process repeated five times to ensure each subset served as the test set, thereby comprehensively assessing the model's performance across different data combinations. Concurrently, the predictive results of the PCA-GA-SVM model were compared with those of the GA-SVM, GA-BP, and PCA-GA-BP models. The GA-SVM and GA-BP models utilized unprocessed raw data, whereas the PCA-GA-SVM and

PCA-GA-BP models used data processed via PCA to reduce redundancy and enhance efficiency. The Back-Propagation Neural Network (BPNN) consists of an input layer, one or more hidden layers, and an output layer, with weights iteratively optimized via the back-propagation algorithm to minimize prediction errors. In the GA-BP model, the genetic algorithm optimizes the initial weights and biases of the BPNN to improve prediction accuracy. The prediction results of the four models are presented in Table 6. The prediction accuracy of each subset in cross-validation is illustrated in Figure 3 (samples 1–7, 8–14, 15–21, 22–29, and 30–37 in different plots).

Table 6: Comparative analysis of prediction results among four models.

Test samples	Actual value	PCA-GA-SVM		GA-SVM		PCA-GA-BP		GA-BP	
		Predicted value	Relative error/%	Predicted value	Relative error/%	Predicted value	Relative error/%	Predicted value	Relative error/%
1	268300.0	264302.3	1.49	254616.7	5.10	236935.7	11.7	208737.4	22.2
2	304900.0	315480.0	3.47	316791.1	3.90	339048.8	11.2	256116.0	16.0
3	83600.00	81627.04	2.36	88825.00	6.25	71979.60	13.9	100905.2	20.7
4	5486.750	5333.670	2.79	5190.470	5.40	4693.910	14.5	4526.570	17.5
5	50314.00	51264.93	1.89	53906.42	7.14	58213.30	15.7	42998.34	14.5
6	106621.0	102676.0	3.70	102686.7	3.69	90734.47	14.9	126612.4	18.8
7	10374.00	10631.28	2.48	9865.670	4.90	11792.13	13.7	8299.200	20.0
8	50490.00	52711.56	4.40	52964.01	4.90	42285.38	16.3	39483.18	21.8
9	14934.00	15240.15	2.05	13799.02	7.60	12992.58	13.0	17323.44	16.0
10	41050.00	39408.00	4.00	43266.70	5.40	35056.70	14.6	31587.98	23.1
11	7020.000	6791.850	3.25	6449.980	8.12	8129.160	15.8	5728.320	18.4
12	139792.0	142434.1	1.89	133109.9	4.78	120640.5	13.7	166702.0	19.3
13	59190.00	56289.69	4.90	63132.05	6.66	69749.50	17.8	49186.89	16.9
14	80649.00	76535.90	5.10	76374.60	5.30	68551.65	15.0	64196.60	20.4
15	41560.00	43949.70	5.75	38401.44	7.60	34162.32	17.8	50786.32	22.2
16	50140.00	49137.20	2.00	51644.20	3.00	42995.05	14.3	42117.60	16.0
17	20272.00	19410.44	4.25	19187.45	5.35	24192.60	19.3	16521.68	18.5
18	33226.00	34089.88	2.60	30528.05	8.12	28042.74	15.6	39572.17	19.1
19	16998.00	16335.08	3.90	16168.50	4.88	14159.33	16.7	13314.53	21.7
20	203759.0	194997.4	4.30	217247.9	6.62	232285.3	14.0	165350.4	18.9
21	189860.0	198783.4	4.70	175392.7	7.62	153786.6	19.0	222895.6	17.4
22	11060.00	10313.45	6.75	9998.240	9.60	9196.390	16.9	8648.920	21.8
23	130800.0	127922.4	2.20	136293.6	4.20	112357.2	14.1	108237.0	17.3
24	446187.0	426554.8	4.40	413838.4	7.25	524715.9	17.6	352933.9	20.9
25	41137.00	43584.65	5.95	36982.16	10.1	34863.61	15.3	49097.01	19.4
26	215400.0	200106.6	7.10	230262.6	6.90	180074.4	16.4	185244.0	14.0
27	238480.0	230133.2	3.50	218566.9	8.35	271867.2	14.0	293616.6	23.1
28	27840.00	29276.54	5.16	25612.80	8.00	22909.54	17.7	23162.88	16.8
29	18322.00	17167.71	6.30	20036.94	9.36	15417.96	15.9	13459.34	26.5
30	199032.0	187587.7	5.75	180024.4	9.55	232071.3	16.6	241823.9	21.5
31	477104.0	487600.3	2.20	457065.6	4.20	410309.4	14.0	397189.1	16.8
32	12099.00	11397.26	5.80	13115.32	8.40	10011.92	17.3	14506.70	19.9
33	6032378	6249544	3.60	5625192	6.75	5124505	15.1	4801772	20.4
34	1758800	1684051	4.25	1581161	10.1	1496739	14.9	1512568	14.0
35	270715.0	286687.2	5.90	250411.4	7.50	316736.6	17.0	333520.9	23.2
36	511020.0	493645.3	3.40	558493.8	9.29	428745.8	16.1	403654.7	21.0
37	269203.0	287508.8	6.80	253589.2	5.80	223815.4	16.9	207286.3	23.0

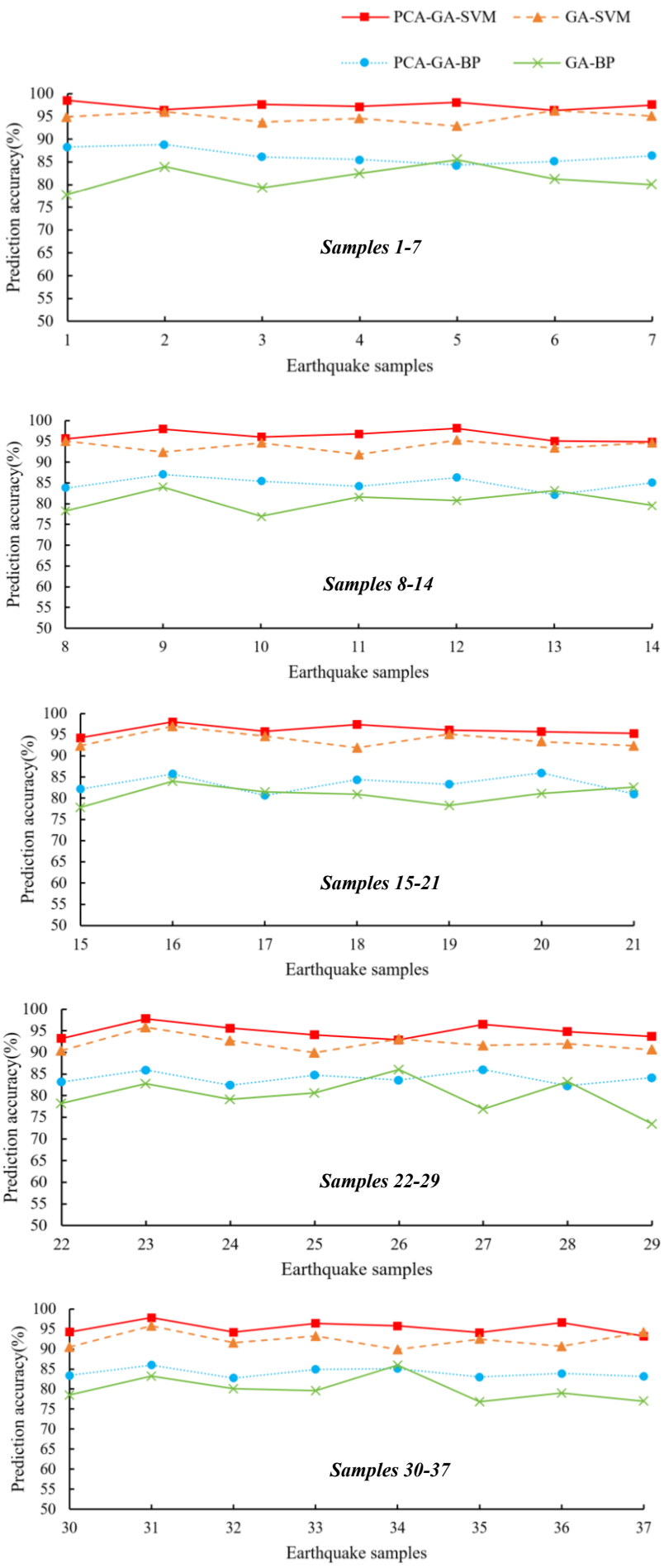

Figure* 3: *The prediction accuracy of the 37 samples.

Based on the prediction results presented in Table 6 and Figure 3, significant differences in prediction accuracy are observed across the four models for various earthquake samples. Among them, the PCA-GA-SVM model exhibits the highest stability and accuracy, maintaining prediction precision above 95% for nearly all samples except a few, with an average prediction accuracy of 95.94%. In contrast, the GA-SVM model demonstrates relatively good performance; however, due to the absence of principal component analysis, its prediction accuracy declines noticeably for certain samples, resulting in an average accuracy of 93.31%. The two BP neural network-based models perform relatively poorly, with the GA-BP model showing the lowest average accuracy of 80.57%, including several samples with prediction errors exceeding 20%; the PCA-GA-BP model, enhanced by the incorporation of PCA, improves to an average accuracy of 84.49%. These findings indicate that SVM exhibits superior generalization ability and stability compared to the BP neural network, particularly for small-sample, high-dimensional nonlinear problems. Additionally, the integration of PCA effectively eliminates redundant information, enhancing both training efficiency and prediction accuracy. Therefore, comprehensively, the PCA-GA-SVM model emerges as the optimal choice for predicting earthquake economic losses in this study, combining high accuracy with robust performance.

Comprehensive Performance Analysis

To further evaluate the reliability of the predictions, a comprehensive analysis of the results from the four models was conducted, employing *MAPE*, *NRMSE*, and R^2 as performance metrics, with the results summarized in Table 7. The comparative performance of the six models, as indicated in Table 7, reveals significant differences in their ability to predict earthquake economic losses. The PCA-GA-SVM model outperforms all others, exhibiting the lowest *MAPE* (4.0522%), the lowest *NRMSE* (2.361%), and the highest R^2 (0.9994), demonstrating excellent accuracy and consistency. The GA-SVM model follows, with a *MAPE* of 4.7968%, an *NRMSE* of 2.612%, and an R^2 of 0.9989. The PCA-GA-BP and GA-BP models show intermediate performance, with *MAPE* values of 12.541% and 16.737%, *NRMSE* values of 6.282% and 7.661%, and R^2 values of 0.9733 and 0.9642, respectively. In contrast, the simple linear and log-linear models perform poorly, with *MAPE* values of 223.35% and 127.36%, *NRMSE* values of 165.3% and 153.0%, and R^2 values of 0.5540 and 0.5710, respectively, highlighting their inability to capture the complex nonlinear relationships within the data. Normalizing the mean square error by the average economic loss provides a relative measure of prediction error. The PCA-GA-SVM model achieves the lowest *NRMSE* (2.361%), indicating that its prediction error constitutes only 2.361% of the average economic loss, compared to 2.612% for GA-SVM, 6.282% for PCA-GA-BP, 7.661% for GA-BP, 165.3% for the simple linear model, and 153.0% for the log-linear model. This underscores the superior performance of the PCA-GA-SVM model in achieving consistent predictions across a wide range of economic losses.

Table 7: Comprehensive analysis of prediction results.

Model	*NRMSE*(%)	*MAPE* (%)	R^2
PCA-GA-SVM	2.361	4.0522	0.9994
GA-SVM	2.612	4.7968	0.9989
PCA-GA-BP	6.282	12.541	0.9733
GA-BP	7.661	16.737	0.9642
Simple Linear	165.3	223.35	0.5540
Log-Linear	153.0	127.36	0.5710

CONCLUSIONS

This study developed and validated a PCA-GA-SVM model for predicting economic losses from earthquakes in mainland China, leveraging the strengths of principal component analysis, genetic algorithm, and support vector machine. The conclusions from each perspective are as follows:

(1) PCA effectively reduces the dimensionality of earthquake loss factors from five indicators (earthquake magnitude, epicentral intensity, seismic design intensity, per capita GDP, and population density) to four principal components, retaining 97.635% of the original data's information. By eliminating components with lower contributions, PCA simplifies the input structure, enhancing computational efficiency without compromising predictive capability. Using PCA-processed data, model accuracy improved by 2.63% (PCA-GA-SVM vs. GA-SVM) and 3.91% (PCA-GA-BP vs. GA-BP), highlighting PCA's role in removing redundant information and boosting model performance.

(2) GA optimization significantly enhanced SVM parameter selection, achieving optimal values of $C = 89.3138$ and $g = 0.012398$ with a low *MSE* of 0.00010988. Unlike empirical tuning, GA's evolutionary approach ensured rapid convergence (after 30 generations) and high fitness, directly contributing to the PCA-GA-SVM model's 95.94% accuracy. This precision in parameter optimization highlights GA's superiority over traditional methods, enabling the SVM to generalize effectively across diverse seismic scenarios.

(3) The SVM framework, enhanced by PCA and GA, outperformed BP neural network models, achieving a 95.94% average prediction accuracy compared to 84.49% (PCA-GA-BP) and 80.57% (GA-BP). Its metrics—*MAPE* (4.0522%), *NRMSE* (2.361%), and R^2 (0.9994)—demonstrate exceptional predictive accuracy and stability, surpassing GA-SVM (93.31%) due to PCA's dimensionality reduction. SVM's robustness in handling small-sample, nonlinear earthquake data, combined with PCA-GA optimization, establishes it as a reliable tool for rapid and accurate economic loss prediction.

ACKNOWLEDGMENTS

This research was supported by Hebei Province Earthquake Science and Technology Spark Project (DZ2025081400001).

REFERENCES

1 Gu Z, Li Y, Zhang M and Liu Y (2023). "Modelling Economic losses from earthquakes using regression forests: Application to parametric insurance". *Economic Modelling*, **125**: 106350. https://doi.org/10.1016/j.econmod.2023.106350

2 Wu J, Li N, Hallegatte S, Shi P, Hu A and Liu X (2012). "Regional indirect economic impact evaluation of the 2008 Wenchuan Earthquake". *Environmental Earth Sciences*, **65**: 161-172. https://doi.org/10.1007/s12665-011-1078-9

3 Zhou S, Zhai G, Shi Y and Lu Y (2020). "Urban seismic risk assessment by integrating direct economic loss and loss of statistical life: an empirical study in Xiamen, China". *International Journal of Environmental Research and Public Health*, **17**(21): 8154. https://doi.org/10.3390/ijerph17218154

4 Guettiche A, Philippe G and Mostefa M (2017). "Economic and human loss empirical models for earthquakes in the Mediterranean region, with particular focus on Algeria". *International Journal of Disaster Risk Science*, **8**: 415-434. https://doi.org/10.1007/s13753-017-0153-6

5 Zhang ZT, Chen Y, Tang H and Chen X (2019). "Allocating assistance after a catastrophe based on the dynamic assessment of indirect economic losses". *Natural Hazards*, **99**: 17-37. https://doi.org/10.1007/s11069-019-03679-0

6 Zhang PZ, Wen X, Shen Z and Chen J (2013). "Active faults, earthquake disasters and their dynamic processes in the mainland of China". *Science China Earth Sciences*, **43**: 1607-1620. https://doi.org/10.1360/zd-2013-43-10-1607

7 Freeman JR (1932). *Earthquake Damage and Earthquake Insurance*. New York: Mc Graw-Hill.

8 Algermissen ST and Steinbrugge KV (1984). "Seismic hazard and risk assessment: some case studies". *Geneva Papers on Risk and Insurance*, **9**(30): 8-26.

9 Xu GD, Liu J, Yu H and Zhao X. (2008). "The fast loss assessment of the Wenchuan Earthquake". *Journal of Earthquake Engineering and Engineering Vibration*, **28**(06): 74-83. https://doi.org/10.13197/j.eeev.2008.06.002

10 Li Z and Wang XQ (2010). "A review of micro and micro-methods for earthquake disaster loss rapid estimation". *Earthquake*, **30**(02): 134-142. https://doi.org/10.3969/j.issn.1000-3274.2010.02.015

11 Chen QF and Chen L (1999). "Vulnerability Analysis in Earthquake Loss Estimate". *Earthquake Research in China*, **15**(2): 97-105. (In Chinese)
CNKI:SUN:ZGZD.0.1999-02-000

12 Liu SQ, Qiu H and Wang XQ (2010). "A rapid earthquake disaster assessment method based on macroeconomic indicators and its implementation". *Journal of Natural Disasters*, **25**(03): 16~19+31. (In Chinese) https://doi.org/10.3969/j.issn.1000-811X.2010.03.004

13 Fan ZW, Yang F and Chen XY. (2016). "Rapid assessment of economic losses after the Zhangjiakou earthquake based on macroeconomic indicators". *Journal of Disaster Prevention and Mitigation*, **32**(03): 15~18. (In Chinese) https://doi.org/10.13693/j.cnki.cn21-1573.2016.03.003

14 Badal J, Vazquez-Prada M and González Á (2005). "Preliminary quantitative assessment of earthquake casualties and damages". *Natural Hazards*, **34**: 353-374. https://doi.org/10.1007/s11069-004-3656-6

15 Wang L, Zhou J, Zhang H and Li Y (2007). "Research and implementation of earthquake damage assessment method for buildings based on remote sensing and GIS". *Earthquake*, **4**: 77~83. (In Chinese) https://doi.org/10.3969/j.issn.1000-3274.2007.04.009

16 Zhou GH, Hong L and Liu C (2013). "Study on the direct economic loss assessment of earthquake buildings based on GIS". *Surveying and Mapping and Spatial Geographic Information*, **36**(10): 56~59. (In Chinese) https://doi.org/10.3969/j.issn.1672-5867.2013.10.017

17 Lu Y and Ding XN (2021). "Application of UAV remote sensing in earthquake disaster loss pre-assessment". *Surveying and Mapping Bulletin*, **S1**: 170-172. (In Chinese) https://doi.org/10.13474/j.cnki.11-246.2021.0538

18 Zhao JP, Li T, Wang J and Xu Y (2024). "Multi-source driven estimation of earthquake economic losses: A comprehensive and interpretable ensemble machine learning model". *International Journal of Disaster Risk Reduction*, **106**: 104377. https://doi.org/10.1016/j.ijdrr.2024.104377

19 Zhang Y, Wu Z, Liu J and Li Q (2023). "Earthquake-induced building damage recognition from unmanned aerial vehicle remote sensing using scale-invariant feature transform characteristics and support vector machine classification". *Earthquake Spectra*, **39**(2): 962-984. https://doi.org/10.1177/87552930231157549

20 Men KP and Lei C (2012). "Research on evaluation models and empirical analysis of Earthquake Disaster Losses in China". *Zeitschrift für Naturforschung A*, **67**(10-11): 534-544. https://doi.org/10.5560/ZNA.2012-0059

21 Ding JW, Lu DG and Cao ZG (2024). "Estimation of earthquake-induced direct economic losses of portfolio buildings based on seismic fragility surface". *Journal of Building Engineering*, **98**: 111290. https://doi.org/10.1016/j.jobe.2024.111290

22 Bhochhibhoya S and Roisha M (2022). "Integrated seismic risk assessment in Nepal". *Natural Hazards and Earth System Sciences*, **22**(10): 3211-3230. https://doi.org/10.5194/nhess-22-3211-2022

23 Niu RQ, Zhang L, Wu H and Ye Z (2014). "Susceptibility assessment of landslides triggered by the Lushan earthquake, April 20, 2013, China". *IEEE Journal of Selected Topics in Applied Earth Observations and Remote Sensing*, **7**(9): 3979-3992. https://doi.org/10.1109/JSTARS.2014.2308553

24 Su YL, Wang Z, Li C and Zhang J (2022). "Hazard assessment of earthquake disaster chains based on deep learning—A case study of Mao County, Sichuan province". *Frontiers in Earth Science*, **9**: 683903. https://doi.org/10.3389/feart.2021.683903

25 Wong L, Comerio MC, Holmes WT and Kelly TE (2005). "Potential losses in a repeat of the 1886 Charleston, South Carolina, earthquake". *Earthquake Spectra*, **21**(4): 1157-1184. https://doi.org/10.1193/1.2083907

26 Wang CH, Zhang XT, Wang XS and Chang GP (2025). "Prediction of earthquake death toll based on principal component analysis, improved whale optimization algorithm, and extreme gradient boosting". *Applied Sciences*, **15**(15): 8660. https://doi.org/10.3390/app15158660

27 Li YL, Xin DH and Zhang ZG (2023). "Estimating the economic loss caused by earthquake in Mainland China". *International Journal of Disaster Risk Reduction*, **95**: 103708. https://doi.org/10.1016/j.ijdrr.2023.103708

28 Dorra EM, Stafford PJ and Elghazouli AY (2013). "Earthquake loss estimation for Greater Cairo and the national economic implications". *Bulletin of Earthquake Engineering*, **11**: 1217-1257. https://doi.org/10.1007/s10518-013-9426-7

29 Fan YY, Zhang HY and Li ZQ (2024). "Seismic economic loss assessment of highway girder bridges using Wenchuan earthquake as a sample". *International Journal of Critical Infrastructures*, **20**(1): 33-55. https://doi.org/10.1504/IJCIS.2024.136292

30 Chen WY and Zhang LM (2022). "An automated machine learning approach for earthquake casualty rate and economic loss prediction". *Reliability Engineering & System Safety*, **225**: 108645. https://doi.org/10.1016/j.ress.2022.108645

31 Li XL, Fang M, Wang J, Zhang H and Wu Y (2018). "Spatiotemporal characteristics of earthquake disaster losses in China from 1993 to 2016". *Natural Hazards*, **94**: 843-865. https://doi.org/10.1007/s11069-018-3425-6

32 Li SQ and Chen YS (2023). "Vulnerability and economic loss evaluation model of a typical group structure considering empirical field inspection data". *International Journal of Disaster Risk Reduction*, **88**: 103617. https://doi.org/10.1016/j.ijdrr.2023.103617

33 Wang JF, Li X, Gong L, Zhang J and Zhou D (2018). "Indirect seismic economic loss assessment and recovery evaluation using nighttime light images–application for Wenchuan earthquake". *Natural Hazards and Earth System Sciences*, **18**(12): 3253-3266. https://doi.org/10.5194/nhess-18-3253-2018

34 Hoyos MC and Silva V (2024). "A database and empirical model for earthquake post-loss amplification". *Earthquake Spectra*, **40**(1): 629-646. https://doi.org/10.1177/87552930231207822

35 Wu GY, Zhang L, Xu Y, Liu H and Li P (2024). "Mult hazard resilience and economic loss evaluation method for cable-stayed bridges under the combined effects of scour and earthquakes". *Engineering Structures*, **314**: 118033. https://doi.org/10.1016/j.engstruct.2024.118033

36 Zeng X, Hu Z, Guo J and Zhang Y (2016). "Application of the FEMA-P58 methodology for regional earthquake loss prediction". *Natural Hazards*, **83**: 177-192. https://doi.org/10.1007/s11069-016-2307-z

37 Montazeri M and Abo El Ezz A (2024). "Earthquake economic loss assessment of existing concrete shear wall residential buildings in Eastern Canada". *Earthquake Engineering and Resilience*, **3**(2): 289-312. https://doi.org/10.1002/eer2.84

38 Weatherill GA, Silva V, Crowley H, Bazzurro P and Rossetto T (2015). "Exploring the impact of spatial correlations and uncertainties for portfolio analysis in probabilistic seismic loss estimation". *Bulletin of Earthquake Engineering*, **13**: 957-981. https://doi.org/0.1007/s10518-015-9730-5

39 Salgado-Gálvez MA, Carreño ML, Cardona OD and Barbat AH (2018). "Probabilistic assessment of annual repair rates in pipelines and of direct economic losses in water and sewage networks: application to Manizales, Colombia". *Natural Hazards*, **93**: 5-24. https://doi.org/10.1007/s11069-017-2987-z